Journal of the European Ceramic Society 21 (2001) 2703–2711

www.elsevier.com/locate/jeurceramsoc

Science of tungstenbronze-type like $Ba_{6-3x}R_{8+2x}Ti_{18}O_{54}$ (R = rare earth) microwave dielectric solid solutions

H. Ohsato*

Nagoya Institute of Technology, Gokiso-Cho, Showa-Ku, Nagoya 466-8555, Japan

Abstract

The crystallography of tungstenbronze-type like $Ba_{6-3x}R_{8+2x}Ti_{18}O_{54}$ solid solutions for microwave dielectric materials applied for mobile phone and base station were studied. The crystal data and crystal structure of the fundamental lattice and supperlattice, and derivation of chemical formula and structural formula are summarized. Fourier map of the fundamental structure showed that oxygen ion positions of TiO_6 octahedra were splitted. This fact proved the tilting of octahedra which is cause of superlattice. The mechanisms of microwave dielectric properties are summarized. Finally, guidelines for the design of the microwave dielectric materials are presented.

Keywords: $Ba_{6-3x}R_{8+2x}Ti_{18}O_{54}$ solid solutions; Internal strain; Microwave dielectric ceramics; Resonator; Tungstenbronze-type crystal structure

1. Introduction

The development of microwave telecommunication technology has been promoted by microwave dielectric ceramics. The tungstenbronze-type like $Ba_{6-3x}R_{8+2x}Ti_{18}O_{54}$ solid solutions as shown in Fig. 1 have been applied in mobile phones because of their high dielectric constant. This compound was reported by Kolar et al.[1,2] as $BaO{\cdot}R_2O_3{\cdot}5TiO_2$ (R = rare earth) compound which was corrected to $BaO{\cdot}R_2O_3{\cdot}4TiO_2$ later. About 10 years before Kolar's report, Bolton[3] had systematically studied the TiO_2-rich region of the $BaO–Nd_2O_3–TiO_2$ ternary system. Following Kolar's work, Kawashima et al.[4] reported the compound in the R = Sm system and Nishigaki et al.[5] found another compound having good properties in the vicinity of $0.15(Ba_{0.95},Sr_{0.05})O/0.15Sm_2O_3/0.7TiO_2$.

Matveeva et al.[6] determined first the crystal structure of $Ba_{3.75}Pr_{9.5}Ti_{18}O_{54}$ based on the fundamental unit cell by single crystal X-ray diffraction. This fundamental structure was confirmed by some researchers: Roth et al.[7] and Ohsato et al.[8] by single crystal X-ray diffraction, Kolar et al.[9] by Rietvelt method and so on. The superlattice with twice fundamental lattice spacing along the c-axis was pointed out by Matveeva et al.[6] and Kolar et al.[9] and was confirmed by an oscillation photograph of the single crystal[10] and by electron diffraction[11]. Ohsato et al.[12] and Rawn et al.[13]) reported the superstructure with TiO_6 octahedral tilting. A different crystal structure with no tilting of TiO_6 octahedra was presented as *Pbam* (No. 55) space group by Azough et al.[11]

This compound was found by Varfolomeev et al.[14] to form solid solutions as $Ba_{6-3x}R_{8+2x}Ti_{18}O_{54}$. Ohsato et al.[15] also suggested the solid-solution formula and determined the solid solution regions for the Nd and Sm systems: $0.0 \leqslant x \leqslant 0.7$ if R = Nd and $0.3 \leqslant x \leqslant 0.7$ if R = Sm. The same solid solution region for the Sm system was also found by Negas et al.[16] With decrease in the ionic radius of R ion, the region of the solid solutions becomes narrower and for Gd and Eu, only $BaO{\cdot}R_2O_3{\cdot}4TiO_2$ appeared.[17]

The dielectric properties as a function of composition x were reported for the Sm and Nd systems by Ohsato et al.[18] and Negas et al.,[16] and for the Pr system by Fukuda et al.[19] Ohsato et al.[20] found the special point with $x = 2/3$ at which the $Q{\cdot}f$ value becomes the highest due to the ordering in the rhombic and pentagonal sites. Valant et al.[21] studied the temperature coefficient of dielectric constants derived from the Clausius-Mosotti equation as a function of the ratio of mean radii (r_A/r_B) of A- and B-site ions. Here, r_A/r_B is correlated to tilting of the TiO_6 octahedra.

In this study, we present crystal data and a crystal structure with tilting octahedra, and discuss the mechanisms of the microwave dielectric properties based on basic science, especially crystallography, and show the guideline for the design of the materials.

* Tel.: +81-52-735-5284; fax: +81-52-735-5294.
E-mail address: ohasto@mse.nitech.ac.jp

0955-2219/01/$ - see front matter
PII: S0955-2219(01)00349-1

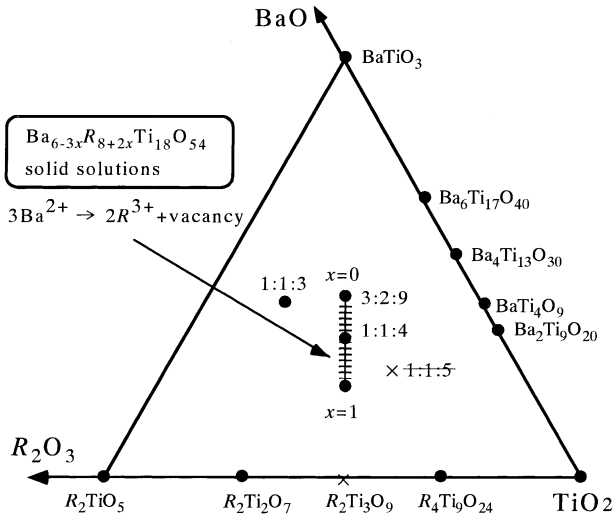

Fig. 1. BaO–R_2O_3–TiO_2 (R = rare earth) ternary system.

2. Experimental

Crystal data were obtained with aid of single crystal X-ray diffraction using the Weissenberg camera and precession camera. The single crystals were grown by self-flux method. The superlattice was found using an oscillation photograph as reported in previous paper.[10]

Crystal structure analysis was performed by using a single crystal four-circle X-ray diffractometer. The ω-2θ scan technique was adopted to collect diffraction intensity data with graphite-monochromatized MoK_α radiation. Three standard reflections showed no significant change during the measurement. The collection range for superlattice was $2\theta < 91°$, $0 \leqslant h \leqslant 24$, $0 \leqslant k \leqslant 44$, $0 \leqslant l \leqslant 13$. 8278 unique reflections were collected among which 6268 reflections with $Fo > 3\sigma(|Fo|)$ were used for the structure analysis. The intensity data with $l = 2n$ for the fundamental lattice were selected from those of superlattice. The initial atomic parameters for the fundamental lattice were used from Matveeva et al.[6] and those of superlattice were derived from those of the fundamental lattice. The intensity data were corrected for Lorentz and polarization factors and absorption. Full-matrix least-squares refinement on F of atomic parameters, with anisotropic thermal parameters and occupations of rare earth ions, was carried out with program *RADY*.[22]

The samples for the measurement of the microwave dielectric properties, the internal strain and lattice parameters were prepared by a solid state reaction as reported in previous papers.[23] The dielectric properties were measured by the Hakki and Colleman method.[24] The samples with optimal $Q{\cdot}f$ values were selected for discussion.

The internal strain η was obtained from the following equation[25] as the grain size of the ceramics is sufficiently large:

$$\beta = 2\eta \tan\theta.$$

Here, β is the full-width at half-maximum (FWHM) of the X-ray powder diffraction peaks. The powder patterns were obtained by multi-detector system (MDS)[26] using synchrotron radiation in the "Photon Factory" of the National Laboratory for High Energy Physics in Tsukuba, Japan. The more precise measuring conditions were reported in previous paper.[27]

Accurate lattice parameters were obtained using the whole-powder-pattern-decomposition method (WPPD) program[28] for the powder diffraction patterns obtained by the step scanning technique using Si (99.99%) as an internal standard.

3. Crystal structure of $Ba_{6-3x}R_{8+2x}Ti_{18}O_{54}$ solid solutions

3.1. Crystal data

Crystal data of both the fundamental lattice and superlattice are shown in Table 1. The naming of the axes is obeyed the rule $b > a > c$ according to the conventional standard. The lattice spacing along the superlattice c-axis is twice that of the fundamental lattice. The morphology of the crystal is needle-like, elongated along the c-axis. Possible space groups of the fundamental lattice and the superlattice include *Pba*2 (No. 32)

Table 1
Crystal data of fundamental lattice and superlattice

Fundamental lattice		Superlattice	
Crystal data		Crystal data	
Chemical formula	$Ba_{6-3x}Sm_{8+2x}Ti_{18}O_{54}$($x = 0.7$)	Chemical formula	$Ba_{6-3x}Sm_{8+2x}Ti_{18}O_{54}$($x = 0.7$)
Crystal lattice type	Orthorhombic	Crystal type	Orthorhombic
Space group	*Pba* 2(No. 32) or *Pbam* (No. 55)	Space group	*Pba* 2_1 (No. 33) or *Pbnm* (No. 62)
a (Å)	12.131(13)	a (Å)	12.131(13)
b (Å)	22.271(5)	b (Å)	22.271(5)
c (Å)	3.819(2)	c (Å)	7.639(5)
Z	1	Z	2
X-ray density (g/cm^3)	5.91	X-ray density (g/cm^3)	5.91

or *Pbam* (No. 55), and $Pbn2_1$ (No. 33) or *Pbnm* (No. 62), respectively. As the result of crystal structural analysis, the space groups *Pbam* and *Pbnm* with center of symmetry were selected for the fundamental lattice and the superlattice, respectively. Recently, Ubic et al.[29] observed extra reciprocal lattice points, and suggested the space group may be $Pb2_1m$ (No. 26), which lacks the *n*-glide plane perpendicular to *b*-axis.

3.2. Crystal structure

The final atomic parameters and *Beq*'s of fundamental structure and superstructure are listed in Tables 2 and 3, respectively. The fundamental structure was converged with space group *Pbam*. The final reliability factor (*R*) is 4.49%. The fundamental structure is composed by three types of large cation sites: ten *A*1 rhombic sites in 2×2 perovskite blocks, four *A*2 pentagonal sites and four trigonal sites. The pentagonal and trigonal sites are located among the perovskite blocks formed by four unit cells of perovskite. Fig. 2 shows a superimposed image of the electron density distribution of the fundamental structure and the framework of superstructure. We found splitting in the oxygen ion positions of TiO_6 octahedra on the Fourier map. The splitting is due to tilting of TiO_6 octahedra as shown in Fig. 3. Therefore, the fundamental structure presents itself a mean structure of the real superstructure which octahedra are tilted along the *c*-axis. The change from the splitting to the tilting corresponds to the symmetry change from 2 to 2_1 along the *c*-axis. Therefore, applying of space group $P2_1/b2_1/a2/m$ (No. 55) to fundamental structure and $P2_1/b2_1/n2_1/m$ (No. 62) to superstructure is considered to be more accurate and convincible. The obtained results, which point out the tilt of TiO_6 octahedra as a main factor for the superlattice formation, precludes the new crystal structure reported by Azough et al.[11] They applied space group *Pbam* (No. 55) to the superstructure. As Ti ions are located on the miller plane, the octahedra stand straight without tilting and with only a little rotation.

Table 2
Coordinations on the fundamental structure of $Ba_{3.87}Sm_{9.4}Ti_{18}O_{54}$ solid solution

Atoms	Site	*g*	*x*	*y*	*z*	*Beq.* (Å)
Ti(1)	2*a*	1.0	0.5	0.5	0.0	0.23(9)
Ti(2)	4*g*	1.0	0.1983(2)	0.4353(1)	0.0	0.14(6)
Ti(3)	4*g*	1.0	0.3976(2)	0.1064(1)	0.0	0.27(6)
Ti(4)	4*g*	1.0	0.1175(2)	0.1634(1)	0.0	0.07(6)
Ti(5)	4*g*	1.0	0.3380(2)	0.2615(1)	0.0	0.09(6)
A 1(1)-Sm	4*h*	0.89	0.19986(9)	0.04815(5)	0.5	0.97(2)
A 1(2)-Sm	2*d*	0.92	0.0	0.5	0.5	0.91(3)
A 1(3)-Sm	4*h*	1.0	0.40687	0.37654(4)	0.5	0.22
A 2-Ba	4*h*	0.968	0.0902(1)	0.30644(6)	0.5	1.23(2)
O(1)	4*h*	1.0	0.100(2)	0.156(2)	0.5	5.4(3)
O(2)	4*g*	1.0	0.418(1)	0.1922(5)	0.0	0.3(3)
O(3)	4*g*	1.0	0.1837(9)	0.2371(6)	0.0	0.9(4)
O(4)	4*h*	1.0	0.333(2)	0.2788(6)	0.5	1.8(3)
O(5)	4*g*	1.0	0.377(1)	0.0193(6)	0.0	0.8(4)
O(6)	4*h*	1.0	0.211(3)	0.4424(8)	0.5	5.2(3)
O(7)	4*g*	1.0	0.242(1)	0.1119(6)	0.0	0.8(4)
O(8)	2*b*	1.0	0.5	0.5	0.5	10.0(6)
O(9)	4*g*	1.0	0.038(1)	0.0811(7)	0.0	6.2(2)
O(10)	4*g*	1.0	0.270(1)	0.3626(6)	0.0	0.9(4)
O(11)	4*g*	1.0	0.345(1)	0.4797(7)	0.0	4.2(1)
O(12)	4*g*	1.0	0.057(1)	0.4032(6)	0.0	4.2(1)
O(13)	4*g*	1.0	0.463(1)	0.3136(6)	0.0	1.6(6)
O(14)	4*h*	1.0	0.398(2)	0.0976(7)	0.5	3.7(3)

3.3. Chemical formula

The distribution of cations in the crystal structure has an important impact on the dielectric properties. To understand more clearly the distribution of the cations, chemical formula and structural formulae are derived. Cations with large ionic radii are located within the three-dimensional framework of $[TiO_6]^{8-}$ octahedra connected at all vertices. The atomic ratio of Ti to O is precisely 1:3 on the framework, and the perovskite-type structure also has this ratio. Then, in the $BaO–R_2O_3–TiO_2$ (R = rare earth) ternary system, the solid solutions with the tungstenbronze-type like structure must be

Table 3
Coordinations on the superstructure of $Ba_{3.87}Sm_{9.4}Ti_{18}O_{54}$ solid solution

Atom	Site	*g*	*x*	*y*	*z*	*Beq.* (Å)
Ti(1)	4*a*	0.5	0.0	0.0	0.0	0.38(5)
Ti(2)	8*d*	1.0	0.19861(11)	0.4352(6)	0.0005(2)	0.29(3)
Ti(3)	8*d*	1.0	0.39783(11)	0.10631(6)	0.0065(2)	0.41(3)
Ti(4)	8*d*	1.0	0.11712(10)	0.16348(5)	0.0026(2)	0.27(3)
Ti(5)	8*d*	1.0	0.33793(10)	0.26155(6)	0.0019(2)	0.31(3)
A 2(1)	4*c*	0.494(1)	0.08528(7)	0.30018(3)	0.25	0.61(2)
A 2(2)	4*c*	0.474	0.59587(7)	0.18661(4)	0.25	0.58(2)
A 1(1)	4*c*	0.396(1)	0.19193(6)	0.04409(3)	0.25	0.39(2)
A 1(2)	4*c*	0.497(1)	0.70581(5)	0.44866(3)	0.25	0.39(2)
A 1(3)	4*c*	0.462(1)	0.99961(6)	0.49402(3)	0.25	0.33(2)
A 1(4)	4*c*	0.501	0.40428(5)	0.37715(2)	0.25	0.34(2)
A 1(5)	4*c*	0.500	0.90971(5)	0.12416(3)	0.25	0.39(2)
O(1)	4*c*	0.5	0.03996(90)	0.17214(37)	0.25	0.58(25)
O(2)	4*c*	0.5	0.60537(72)	0.37016(35)	0.25	0.37(21)
O(3)	8*d*	1.0	0.41821(51)	0.19255(24)	0.0062(10)	0.57(16)
O(4)	8*d*	1.0	0.68511(49)	0.26288(26)	0.0219(8)	0.36(16)
O(5)	4*c*	0.5	0.31213(79)	0.27916(40)	0.25	0.59(25)
O(6)	4*c*	0.5	0.84572(78)	0.22324(42)	0.25	0.51(24)
O(7)	8*d*	1.0	0.37717(57)	0.01829(25)	0.0161(10)	0.70(18)
O(8)	4*c*	0.5	0.23752(83)	0.44275(41)	0.25	0.61(26)
O(9)	4*c*	0.5	0.67319(84)	0.05498(40)	0.25	0.54(24)
O(10)	8*d*	1.0	0.24173(48)	0.11149(26)	0.0215(9)	0.40(15)
O(11)	4*c*	0.5	0.48205(91)	0.4790(41)	0.25	0.66(27)
O(12)	8*d*	1.0	0.3748(59)	0.08057(28)	0.0487(11)	0.83(19)
O(13)	8*d*	1.0	0.76984(54)	0.13784(28)	0.0164(10)	0.71(18)
O(14)	8*d*	1.0	0.84388(52)	0.02003(31)	0.0376(10)	0.65(18)
O(15)	8*d*	1.0	0.05592(50)	0.40400(28)	0.0426(9)	0.51(16)
O(16)	8*d*	1.0	0.46402(48)	0.31258(29)	0.0245(9)	0.52(17)
O(17)	4*c*	0.5	0.42941(104)	0.10066(42)	0.25	0.85(29)
O(18)	4*c*	0.5	0.87883(85)	0.40424(45)	0.25	0.67(26)

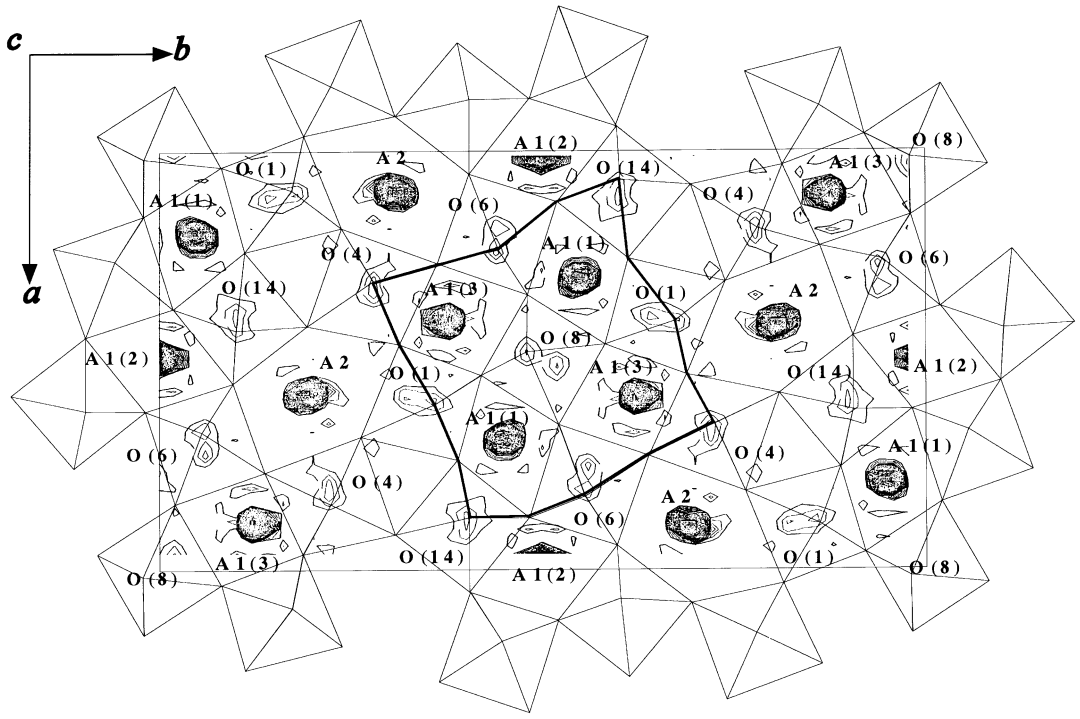

Fig. 2. Electron density map (Fourier map) of the fundamental structure at $z=0.5$ revealing the top oxygen ion separated into two and superimposed a superstructure framework.

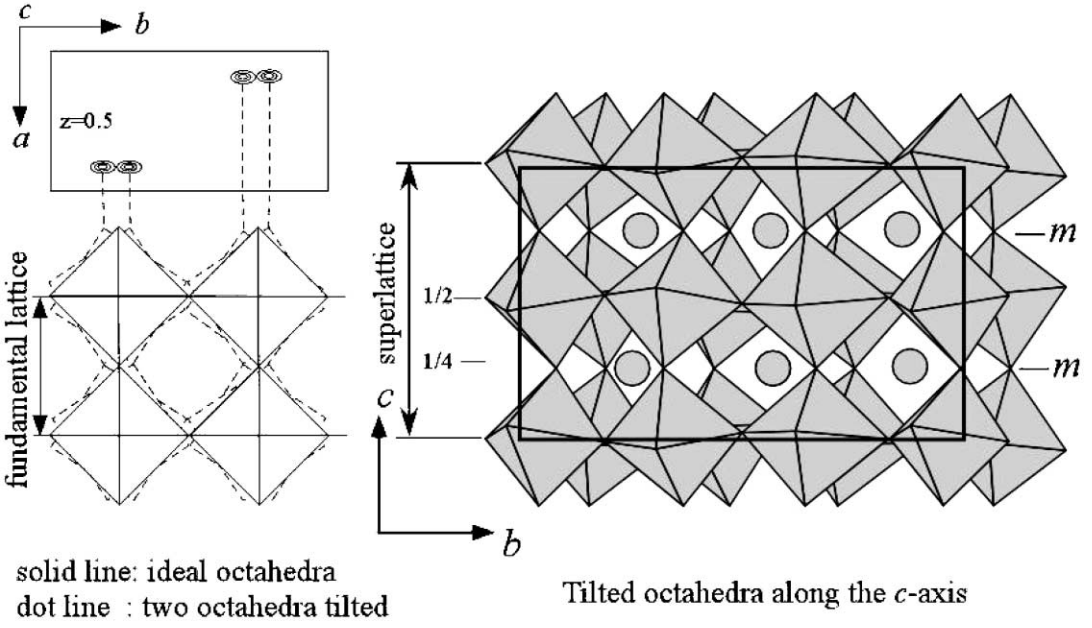

Fig. 3. TiO_6 octahedron tilting deduced from splitting of oxygen ion on the fundamental structure.

formed on the tie line between $BaTiO_3$–$R_2Ti_3O_9$ where Ti/O ratio stays 1:3. $BaO{\cdot}R_2O_3{\cdot}4TiO_2$ also locates on the tie line. Such solid solutions have different valence cations with large size: divalent Ba^{2+} and trivalent rare earth R^{3+}. To maintain electrostatic stability, three Ba^{2+} ions should be replaced with two R^{3+} ions and a vacancy. The substitutional formula of the solid solutions is considered as follows on this tie line.

$$3Ba^{2+} \Longleftrightarrow 2R^{3+} + V_{A1}$$

The derived chemical formula for the solid solutions is as follows:

$$Ba_{6-3x}R_{8+2x}Ti_{18}O_{54}.$$

Here, the formula $Ba_6R_8Ti_{18}O_{54}$ is obtained as the end member of the solid solutions, in which the large

sites: $A1$ rhombic sites and $A2$ pentagonal sites (more detailed description of sites is presented in the previous section) are fully occupied. There is one formula unit in the fundamental unit cell which contains 18 Ti^{4+} ions and 54 O^{2-} ions. The $BaO{\cdot}R_2O_3{\cdot}4TiO_2$ composition corresponds exactly to $x=0.5$, and $Ba_{3.75}Pr_{9.5}Ti_{18}O_{54}$ to $x=0.75$.

There are three different cations with different diameter in the crystal structure, which occupy different sites. The middle-sized R ions mainly occupy the $A1$-sites and the largest Ba ions mainly occupy pentagonal $A2$-sites. If the composition is Ba rich, small amount of Ba ions occupy also $A1$-sites. The smallest Ti ions alone occupy octahedra B-sites. The trigonal C-sites are empty.

The solid solution regions are $0.0 \leqslant x \leqslant 0.7$ for $R=$La, Pr and Nd, and $0.3 \leqslant x \leqslant 0.7$ for $R=$Sm. In the La, Pr and Nd system, the substitution mode of cations undergoes some changes.

3.4. Structural formula

The basic structural formula is as follows:

$$[S_{10}]_{A1}[S_4]_{A2}B_{18}X_{54}$$

Ten S sites in $A1$ and four S sites in $A2$ are included in a fundamental unit cell. Here, B is a cation in an octahedron and X is an anion, occupied by Ti and O ions, respectively. The final composition $Ba_6R_8Ti_{18}O_{54}$ of the solid solutions with $x=0$ is represented as the structural formula $[R_8Ba_2]_{A1}[Ba_4]_{A2}Ti_{18}O_{54}$ in which the two largest Ba ions together with eight middle-sized R ions occupy $A1$-sites. The $A2$-sites are occupied only by four Ba ions. The structural formula of the solid solution is derived as follows from the terminal composition according to the substitution mode $3Ba^{2+} \Longleftrightarrow 2R^{3+} + V_{A1}$.

$$[R_{8+2x}Ba_{2-3x}V_x]_{A1}[Ba_4]_{A2}Ti_{18}O_{54}$$
in the range of $0 \leqslant x \leqslant 2/3$

When all the Ba ions in $A1$-sites are substituted by R ions, $x=2/3$. Moreover, for $x \geqslant 2/3$, Ba ions in $A2$-sites become substituted by R ions, which occupy the $A1$-sites, and vacancies can be created in $A2$-sites. The structural formula is as follows:

$$[R_{9+1/3+2(x-2/3)}V_{2/3-2(x-2/3)}]_{A1}[Ba_{4-3(x-2/3)}V_{3(x-2/3)}]_{A2}$$
$Ti_{18}O_{54}$ in the range of $2/3 \leqslant x \leqslant 1$.

The structural formulae derived above, divide the large cation sites into two kinds: rhombic and pentagonal sites. In the more precise fundamental structure, the $A1$ site separates into three sites as follows:

$$[S_2]_{A11}[S_2]_{A12}[S_2]_{A13}[S_2]_{A2}B_{18}X_{54},$$

and in the real superstructure, $A1$ sites separate into five sites, and $A2$ sites separate into two sites as follows:

$$[S_2]_{A11}[S_2]_{A12}[S_2]_{S13}[S_2]_{A14}[S_2]_{A15}[S_2]_{A21}[S_2]_{A22}B_{18}X_{54}.$$

The site occupancies obtained at $x=0.7$ are represented as follows:

$$[Sm_{1.58}]_{A11}[Sm_{1.99}]_{A12}[Sm_{1.85}]_{A13}[Sm_{2.00}]_{A14}[Sm_{2.00}]_{A15}$$
$$[Ba_{1.98}]_{A21}[Ba_{1.90}]_{A22}Ti_{18}O_{54}$$

In the case of $x=0.5$ the precise structural formula is as follows:

$$[Sm_{1.68}]_{A11}[Sm_{1.96}]_{A12}[Sm_{1.88}]_{A13}[Sm_{1.68}Ba_{0.31}]_{A14}$$
$$[Sm_{1.80}Ba_{0.18}]_{A15}[Ba_{2.00}]_{A21}[Ba_{2.00}]_{A22}Ti_{18}O_{54}$$

The $A14$ and $A15$ sites are occupied by Sm and Ba ions disorderly. As the determination of the site occupancy is difficult, some researchers reported different results as follows:

$$[Sm_{1.72}]_{A11}[Sm_{2.00}]_{A12}[Sm_{0.81}Ba_{1.19}]_{A13}[Sm_{2.00}]_{A14}$$
$$[Sm_{2.00}]_{A15}[Ba_{2.00}]_{A21}[Ba_{2.00}]_{A22}Ti_{18}O_{54}$$
$x = 0.27$ by Rawn et al.[13]

and

$$[Sm_{1.44}Ba_{0.24}]_{A11}[Sm_{1.99}]_{A12}[Sm_{1.65}Ba_{0.26}]_{A13}[Sm_{1.94}]_{A14}$$
$$[Sm_{2.00}]_{A15}[Ba_{2.00}]_{A21}[Ba_{2.00}]_{A22}Ti_{18}O_{54}$$
$x = 0.5$ by Okudera et al.[30]

4. Properties and structure

4.1. High quality factor due to ordering of Ba and R

The dielectric properties as a function of the composition x for the $Ba_{6-3x}R_{8+2x}Ti_{18}O_{54}$ solid solutions[18,20] are shown in Fig. 4. Similar results for Sm and Nd system are shown by Negas et al.[16] The characteristic phenomenon is that $Q{\cdot}f$ values varied non linearly as a function of composition, though ε_r and τ_f vary proportional to the composition. The data of the $x=2/3$ composition in which R and Ba ions occupy separately the rhombic sites ($A1$) and the pentagonal sites ($A2$), respectively, show the highest $Q{\cdot}f$ values: 10549 GHz in the Sm system, 10010 GHz in the Nd system and 2024 GHz in the La system as shown in Fig. 4. The highest quality factor may be based on the ordering of R and Ba ions in the $A1$ and $A2$ sites, respectively. The distribution of the ions might reduce the internal strain and result in the non-linear variation of quality factor.

Internal strain η values for $x=0.3$, 0.5, 2/3 and 0.7 are shown in Fig. 5. It should be noticed that the internal strain for $x=2/3$ is the lowest in the series of $Ba_{6-3x}Sm_{8+2x}Ti_{18}O_{54}$ solid solutions. This low internal strain comes from the distribution of cations in the rhombic sites and the pentagonal sites on the tungstenbronze-

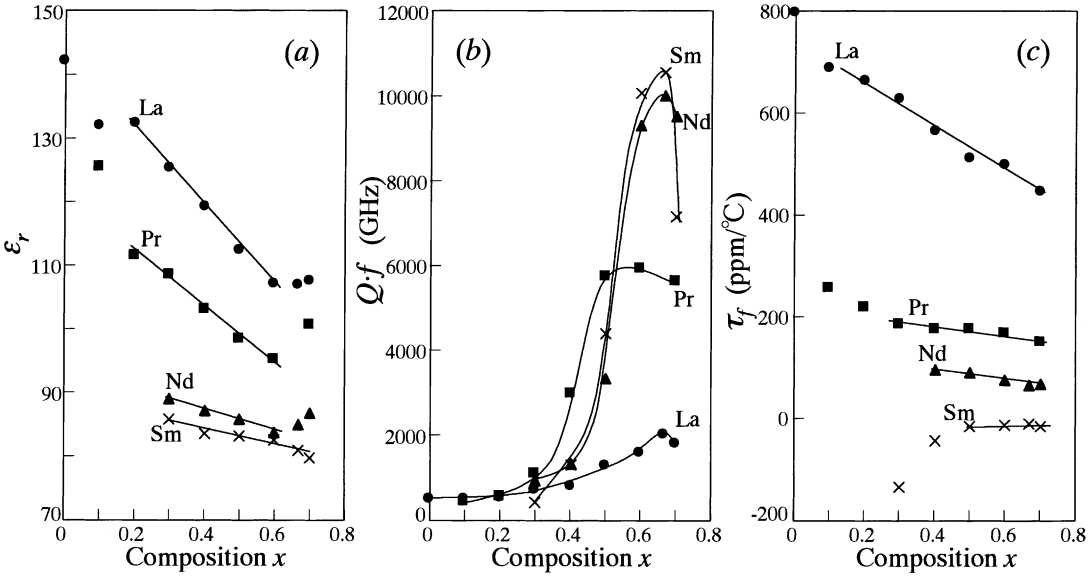

Fig. 4. Dielectric properties of the tungstenbronze-type like $Ba_{6-3x}R_{8+2x}Ti_{18}O_{54}$ solid solutions as a function of composition.

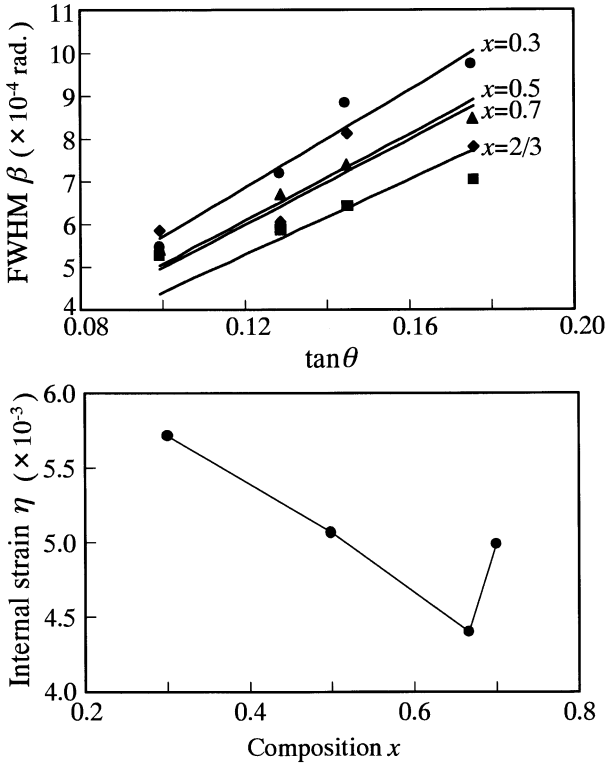

Fig. 5. Internal strain obtained from the equation $\beta = 2\eta\tan\theta$ using FWHM of powder XRD (a), and internal strain vs. composition (b).

type like structure. In the $x=2/3$ composition, ions with the same size occupy each $A1$ and $A2$ site, as shown in the structural formula $[R_{9.33}V_{0.67}]_{A1}[Ba_4]_{A2}Ti_{18}O_{54}$, that means, R ions and Ba ions are ordering in both the rhombic sites and pentagonal sites, respectively. This ordering leads to the lowest strain. As the x-values decrease according to the structural formula $[R_{8+2x}Ba_{2-3x}V_x]_{A1}[Ba_4]_{A2}Ti_{18}O_{54}$ in the range of $0 \leqslant x \leqslant 2/3$, Ba ions with larger ionic radii will occupy also a part of the rhombic sites with their smaller size. The occupation of Ba ions in $A1$ site leads to internal strain around themselves which lowers the $Q{\cdot}f$ values. Moreover, the vacancies generated in $A1$ sites by the substitution of 3Ba by $2R$ might be the second reason for lowering the internal strain and lead to the high $Q{\cdot}f$ values. On the other hand, as the x-values increase according to the structural formula $[R_{9.33+2(x-2/3)}V_{0.66-(x-2/3)}]_{A1}[Ba_{4-3(x-2/3)}V_{3(x-2/3)}]_{A2}Ti_{18}O_{54}$ in the range of $2/3 \leqslant x \leqslant 0.7$, Ba ions in $A2$ sites are substituted by R ions. The decrease of Ba ions produces vacancies in $A2$ sites and may lead to unstable crystal structures, as shown by the limit of solid solubility located near the $x=0.7$ composition. Moreover, the decrease in the number of vacancies in the rhombic sites accompanied by the decrease of Ba ions in the pentagonal sites might lead to an additional internal strain. These strains are the reason for the lower quality factor at the $x=0.7$.

On the other hand, the $Q{\cdot}f$ values of each R-compound with $x=2/3$ in the $Ba_{6-3x}R_{8+2x}Ti_{18}O_{54}$ solid solutions increase according to a decrease in the rare-earth ion size (lanthanoid contraction). The Sm-compound has a better $Q{\cdot}f$ than the La-compound. This crystal structure is maintained by the size difference of large cations such as Ba and R. It was revealed that the crystal structure with the largest size difference between Ba and R shows excellent quality factor, as it has low internal strain.

4.2. Dielectric constant and temperature coefficient of resonant frequency

The dielectric constant (ε_r) is affected by the following three effects: (I) volume of TiO_6 octahedra, (II) tilting of

Table 4
Volume and tilt angles of TiO_6 octahedra strings along the c-axis about two compositions of $x=0.5$ and 0.7

	x	Ti(1)	Ti(2)	Ti(3)	Ti(4)	Ti(5)	Mean
Volume (Å^3)	0.5	9.864	10.04	9.791	9.737	10.30	9.946
	0.7	9.858	10.04	9.777	9.761	10.19	9.925
Tilt angle (θ)	0.5	14.45	10.80	8.996	10.03	5.672	9.990
	0.7	15.10	11.56	9.261	11.07	6.161	10.63

octahedra strings and (III) polarizabilities of R and Ba ions. The dielectric constants of the solid solutions are proportional to lattice parameters or cell volumes as shown in Fig. 7a. As x increased, ε_r decreased linearly and lattice parameters or cell volumes also decreased linearly.[20]

Usually, in the perovskite structure, the polarity of the Ti ion in the octahedra is produced as a result of the large octahedral volume. Thus, as the mean value of the volume decreased from 9.946 Å^3 at $x=0.5$ to 9.925 Å^3 at $x=0.7$ as shown in Table 4, this volume change is considered to have decreased ε_r. However, the volume change is very small, thus other effects should be examined, such as tilting of the TiO_6 octahedra strings as suggested by Valant et al.[21] The tilting angle, which is between the c-axis and the central axis of the octahedra as shown in Fig. 6, is inverse proportional to lattice parameters: the mean tilting angle is 9.99° at $x=0.5$ and 10.65° at $x=0.7$, based on the refined crystal structure of the Sm solid solution series as shown in Table 4.

ε_r and τ_f for the solid solution regions with $0.3\leqslant x\leqslant 0.7$ for the Sm system, $0\leqslant x\leqslant 0.7$ for the Nd, Pr and La systems are replotted as a function of unit cell volume in Fig. 7. These ε_r and τ_f values are almost proportional to the unit cell volume. The size of cell volume affects to the ε_r such as large size brings large ε_r. From this figure, it was also deduced that the polarizabilities of R ions affect ε_r and τ_f. On the table of the polarizabilities derived by Shannon,[31] the La ion, which gives the largest ε_r in the series, also has the largest polarisability among these R ions: 6.03 for La, 5.31 for Pr, 5.01 for Nd and 4.74 Å^3 for Sm. The ε_r values decrease with the polarizabilities. On the other hand, the ε_r values also vary linearly as a function of cell volume in each R-system as shown in Fig. 7a. The variations of ε_r are also affected by the polarizabilities of R and Ba ions. The substitution is performed according to the following equation: $3Ba\rightarrow 2R+V$. The total polarizabilities due to the substitution equation are reduced from 3×6.40 to 2×6.03 Å^3 for the La system. Here, the value of 6.40 Å^3 for the Ba^{+2} ion is larger than that for the La^{+3} ion.

The τ_f are also plotted as a function of cell volume in Fig. 7b. Though similar tendency with ε_r is observed, the mechanism of τ_f has not been clarified yet. The τ_f values of the Sm system are usually negative but close to zero. As τ_f obeys additional rule, we could get easily a material with the $\tau_f=0$ ppm/°C. In the Sm system adding Nd or La system, outstanding materials with $\tau_f=0$ ppm/°C have been realized by Ohsato.[32]

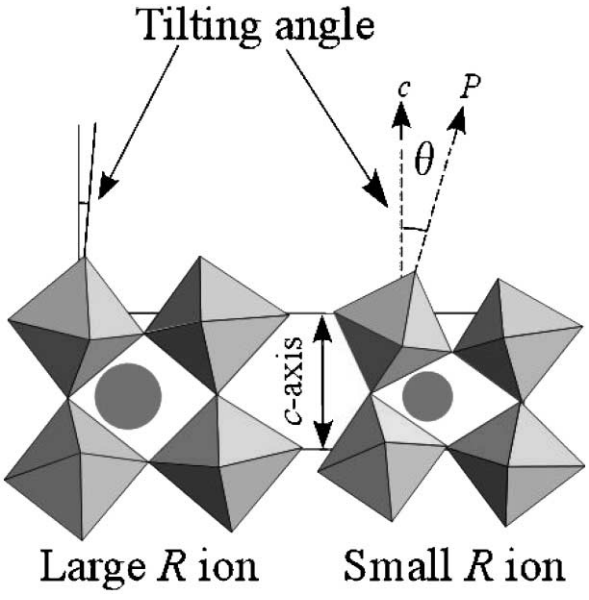

Fig. 6. Dielectric constant ε_r concerned with tilting angle.

5. Guidelines for the design of the materials

1. Knowledge of the crystal structure is basically very important, such as super structure, ordering and distribution of cations, for the development of high $Q{\cdot}f$

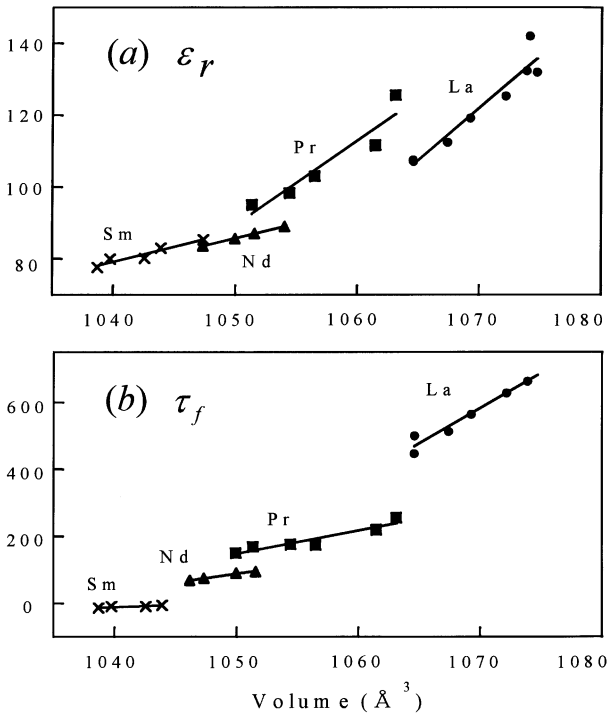

Fig. 7. The dielectric constant (a) and the temperature coefficients of resonant frequency (b) as a function of the unit cell volume.

ceramics. 2. Selection of the structure without internal strain for high Q (low loss) dielectric materials. The internal strain is reduced by ordering of cations. In this case, ordering composition of Ba and R ions at $x=2/3$ brings low internal strain and high Q. 3. Crystal structure with centrosymmetry is better for high $Q{\cdot}f$. 4. For high ε_r or high polarity, selection of large octahedral volume, and small tilting angle. These factors are found for these solid solution series. 5. For high ε_r, selection of atoms with large polarizability values proposed by Shannon.[31] The ε_r increases with polarizability: Eu (4.53)⇒Sm (4.74)⇒Nd (5.01)⇒Pr (5.31)⇒(6.03)⇒Ba(6.40) Å^3. 6. Value of τ_f = zero ppm/°C could be achieved by additive rule using the materials with positive and negative τ_f or making solid solutions between composition with positive and negative τ_f. The example is shown in the Sm–Nd and Sm–La systems.[32]

6. Summary

The space groups, which were presented by many researchers, were confirmed as *Pbam* for fundamental lattice and *Pbnm* for superlattice. The crystal structure is refined as tungstenbronze-type like structure with 2×2 perovskite blocks by X-ray crystal structure analysis. The superstructure is caused by the tilting of octahedra strings along the *c*-axis which was deduced from splitting of oxygen ion position on the Fourier map of the fundamental lattice. The chemical and structural formulae were derived. Mechanisms of dielectric properties are stated, and ordering of Ba and R ions at $x=2/3$ composition is considered to result in high quality factors. The dielectric constants are found to be affected by three kinds of factors: volume of octahedron, tilting of octahedron and polarizabilities of ions. Finally, guidelines for the design of dielectric materials are suggested.

Acknowledgements

The authors would like to thank Dr. S. Nishigaki, Mr. A. Harada, Mr. M. Imaeda, Mr. H. Sakashita and Dr. A. Kirianov. This work was supported in part by a Grant-in Aid for Science Research (B) from the Ministry of Education, Science, Sports and Culture, and the author is also supported by The Dispatch Scholarship 2000 for attendance at in the MMA 2000 (International Conference on Microwave Materials and Their Applications).

References

1. Kolar, D., Stadler, Z., Gaberscek, S. and Suvorov, D., Ceramic and dielectric properties of selected compositions in the BaO-TiO_2-Nd_2O_3 system. *Ber. Dt. Keram. Ges.,* 1978, **55**, 346–347.
2. Kolar, D., Gaberscek, S. and Volavsek, B., Synthesis and crystal chemistry of $BaNdTi_3O_{10}$, $BaNd_2Ti_5O_{14}$, and $Nd_4Ti_5O_{24}$. *J. Solid State Chem.,* 1981, **38**, 58–164.
3. Bolton, R. L., Temperature Compensating Ceramic Capacitors in the System Baria–Rare-earth-oxide Titania. PhD thesis, Ceramic Engineering, University of Illinois, Urbana, IL, (University Microfilms International, A Bell & Howell Information Company), 1968.
4. Kawashima, S., Nishida, M., Ueda, I. and Ouchi, H., Dielectric Properties at Microwave Frequencies of the Ceramics in BaOS-$m_2O_3TiO_2$ System. Presented at the 87th Annual Meeting, American Ceramic Society, Cincinnati, OH, 6 May 1985 (Electronics Division Paper No.15-E-85).
5. Nishigaki, S., Kato, H., Yano, S. and Kamimura, R., Microwave dielectric properties of (Ba,Sr)O–Sm_2O_3–TiO_2 ceramics. *Am. Ceram. Soc. Bull.,* 1987, **66**, 1405–1410.
6. Matveeva, R. G., Varforomeev, M. B. and ll'yuschenko, L. S., Refinement of the composition crystal structure of $Ba_{375}Pr_{95}$-$Ti_{18}O_{54}$. *Zh. Neorg. Khim.,* 1984, **29**, 31–34 (trans. Russ. J. Inorg. Chem., 1984, **29**, 17-19.).
7. Roth, R. S., Beach, F., Antoro, A., Davis, K. and Soubeyroux, J. L., Structural of the nonstoichiometric solid solutions $Ba_2RE_4[Ba_x+RE_{2/3-2/3x}]Ti_9O_{27}$(RE = Nd,Sm). *14 Int. Congress Crystallog, Collected Abst*., 1987, 07. 9-9, Perth, Australia.
8. Ohsato, H., Ohhashi, T. and Okuda, T., Structure of $Ba_{6-3x}Sm_{8+2x}Ti_{18}O_{54}$ ($0<x<1$). Ext. Abstr. AsCA '92 Conf., Singapore, November, 1992, 14U-50.
9. Kolar, D., Gabrscek, S. and Suvorov, D., Structural and dielectric properties of perovskite- like rare earth titanates. *Third Euro-Ceramics,* 1993, **2**, 229–234.
10. Ohsato, H., Nishigaki, S. and Okuda, T., Superlattice and dielectric properties of dielectric compounds. *Jpn. J. Appl. Phys.,* 1992, **31**, 3136–3138.
11. Azough, F., Setasuwon, P. and Freer, R., The structure and microwave dielectric propreties of ceramics based on $Ba_{3.75}Nd_{9.5}Ti_{18}O_{54}$.. *Materials and Processes for Wireless Communications. Ceram Trans.,* 1995, **53**, 215–226.
12. Ohsato, H., Kato, H., Mizuta, M., Nishigaki, S. and Okuda, T., Superstructure of $Ba_{6-3x}Sm_{8+2x}Ti_{18}O_{54}$ ($x=0.71$). Ext. Abstr. AsCA'95 *Conf*., Thailand, November 1995, 1P40.
13. Rawn, C. J., Birnie III, D. P., Bruck, M. A., Enemark, J. H. and Roth, R. S., Structural investigation of $Ba_{6-3x}Ln_{8+2x}Ti_{18}O_{54}$ ($x=0.27$, Ln = Sm) by single crystal X-ray diffraction in space group *Pnma* (No.62). *J. Mater. Res.,* 1998, **13**(1), 187–196.
14. Varfolomeev, M. B., Mironov, A. S., Kostomarov, V. S., Golubtsova, L. A. and Zolotova, T. A., The synthesis and homogeneity ranges of the phases $Ba_{6-x}R_{8+2x/3}Ti_{18}O_{54}$.. *Russ. J. Inorg. Chem.,* 1988, **33**, 607–608.
15. Ohsato, H., Ohhashi, T., Nishigaki, S., Okuda, T., Sumiya, K. and Suzuki, S., Formation of solid solution of new tungsten bronze-type microwave dielectric compounds $Ba_{6-3x}R_{8+2x}Ti_{18}O_{54}$ (R = Nd and Sm, $0\leqslant x\leqslant 1$). *Jpn. J. Appl. Phys.,* 1993, **32**, 4323–4326.
16. Negas, T. and Davies, P. K., Influence of chemistry and processing on the electrical properties of $Ba_{6-3x}Ln_{8+2x}Ti_{18}O_{54}$ solid solutions. *Material and Processes for Wireless Communications. Ceramic Transactions.,* 1995, **53**, 196–197.
17. Valant, M., Suvorov, D. and Kolar, D., X-ray investigations and dielectric property determination of the $Ba_{4.5}Gd_9Ti_{18}O_{54}$ compound. *Jpn. J. Appl. Phys.,* 1996, **35**, 144–150.
18. Ohsato, H., Ohhashi, T., Kato, H., Nishigaki, S. and Okuda, T., Microwave dielectric properties and structure of the $Ba_{6-3x}Sm_{8+2x}Ti_{18}O_{54}$ solid solutions. *Jpn. J. Appl. Phys.,* 1995, **34**, 187–191.
19. Fukuda, K., Kitoh, R. and Awai, I., Microwave characteristics of mixed phases of $BaPr_2Ti_4O_{12}$-$BaPr_2Ti_5O_{14}$ ceramics. *J. Mater. Res.,* 1995, **10**, 312–319.

20. Ohsato, H., Mizuta, M., Ikoma, T., Onogi, Z., Nishigaki, S. and Okuda, T., Microwave dielectric properties of tungsten bronze-type $Ba_{6-3x}R_{8+2x}Ti_{18}O_{54}$ (R = La, Pr, Nd and Sm) solid solutions. *J. Ceram. Soc. Japan,* 1998, **106**(2), 178–182.
21. Valant, M., Suvorov, D. and Rawn, C. J., Intrinsic reasons for variations in dielectric properties of $Ba_{6-3x}R_{8+2x}Ti_{18}O_{54}$ (R = La-Gd) solid solutions. *Jpn. J. Appl. Phys.,* 1999, **38**, 2820–2826.
22. Sasaki, S., A Fortran Program for the Least-squares Refinement of Crystal Structures. XL Report, ESS, State University of New York, 1982, pp. 1–17.
23. Mizuta, M., Uenoyama, K., Ohsato, H., Nishigaki, S. and Okuda, T., Formation of the tungusten bronze-type $(Ba_{6-3x}Sm_{8+2x})_{\alpha}$-$Ti_{18-y}Al_yO_{54}$($\alpha = 1 + y/36$) solid solutions, microwave dielectric properties. *Jpn. J. Appl. Phys.,* 1996, **35**, 5065–50687.
24. Hakki, B. W. and Coleman, P. D., A dielectric resonator method of measuring inductive in the millimeter range. IRE Trans. Microwave Theory & Tech., 1960, MTT-8, 402–410.
25. Stokes, A. R. and Willson, A. J. C., The diffraction of X-rays by distorted crystal aggregates-I. *Proc. Phys. Soc.,* 1944, **56**, 174–181.
26. Toraya, H., Hibino, H. and Ohsumi, K., A new powder diffractometer for synchrotron radiation with multiple-detector system. *J. Synchrotron Rad.,* 1996, **3**, 75–83.
27. Ohsato, H., Imaeda, M., Takagi, Y., Komura, A. and Okuda, T., Microwave quality factor improved by ordering of Ba and rare-earth on the tungstenbronze-type $Ba_{6-3x}R_{8+2x}Ti_{18}O_{54}$ (R = La, Nd and Sm) solid solutions. In *Proceeding of the XIth IEEE International Symposium on Applications of Ferroelectrics,* 1998, IEEE catalog number 98CH36245, pp. 509–512.
28. Toraya, H., Whole-powder-pattern fitting without reference to a structural model: application to X-ray powder diffractometer Data. *J. Appl. Cryst.,* 1986, **19**, 440–447.
29. Ubic, V., Reaney, I. M. and Lee, W. E., Space group determination of $Ba_{6-3x}Sm_{8+2x}Ti_{18}O_{54}$. *J. Am. Ceram. Soc.,* 1999, **82**, 1336–1338.
30. Okudera, H., Nakamura, M., Toraya, H. and Ohsato, H., Tungsten bronze-type solid solutions $Ba_{6-3x}R_{8+2x}Ti_{18}O_{54}$ (x = 0.3, 0.5, 0.67, 0.71) with superstructure. *J. Solid State Chem.,* 1999, **142**, 336–343.
31. Shannon, R. D., Dielectric polarizabilities of ions in oxides and fluorides. *Jpn. J. Appl. Phys.,* 1993, **73**, 348–366.
32. Ohsato, H., Kato, H., Mizuta, M., Nishigaki, S. and Okuda, T., Microwave dielectric properties of the $Ba_{6-3x}(Sm_{1-y}R_y)_{8+2x}$-$Ti_{18}O_{54}$ (R = Nd, La) solid solutions with zero temperature coefficient of the resonant frequency. *Jpn. J. Appl. Phys.,* 1995, **34**, 5413–5417.